

Figure 3. Three-dimensional plots of STO-3G//6-31G* wave functions calculated with the PSI/77 program (ref 30): (a) 3-cyanocyclopropene; (b) cyclopropene.

We propose that (relative to **3**) a reduced cyclopropenyl $2b_2$ (π) \leftrightarrow $\sigma(C_3C_4)$ four-electron repulsion (Figure 2b) coupled with an enhanced cyclopropenyl $2b_2$ (π) \rightarrow $\sigma^*(C_3C_4)$ donation (Figure 2c) make a significant contribution to the ground state of **1**. It can be seen that the second of these effects leads directly to a relative lengthening of C_1C_2 and C_3C_4 and a shortening of C_1C_3 which counterbalances the cyano $3b_1 \rightarrow$ cyclopropenyl π^* effects.

This interpretation is supported by the fact that the C_1C_2 π -electron density in **1** is calculated at the 6-31G* level to be 0.014 electron less than that in **3** whereas the total cyano electron density in **1** is 0.007 electron greater than that in **2**. The observation that the CCN unit is calculated to bend slightly away from C_1H in

2 but slightly toward C_3H in **1** is also consistent with this interpretation.

The result of this mixing is illustrated by three-dimensional orbital plots of the HOMOs of **1** and **3**. The wave function at C_3 in **3** (Figure 3b) is moderately large owing to a dominant antibonding mixing of the C_1C_2 π orbital with the CH_2 pseudo- π orbital. In contrast, the corresponding orbital in **1** (Figure 3a) has a smaller contribution from the HC_3CN orbitals. This is consistent with a reduced mixing with $\sigma(HC_3CN)$ and an increased mixing with $\sigma^*(HC_3CN)$ compared to the corresponding orbitals in **3**. Since these mixings offset each other at C_3 , the dominant mixing with $\sigma(HC_3H)$ calculated for **3** is attenuated in **1**. This explanation is supported by the fact that the ring π orbital for **1** is calculated to be 1.29 eV lower in energy than that for **3**.

In summary, we conclude that, although the distortion of the three-membered ring in **1** relative to **3** is much less than the corresponding distortion in **2** relative to **4**, there is actually *more* conjugation (and less repulsion) between the cyano group and the ring in **1** than in **2**. Interaction a in Figure 2 is probably present in **1** to an extent comparable to that in **2**, but its structural effect is attenuated by a reduction in interaction b and by an increase in interaction c. This once again illustrates the importance of *both* stabilizing two-electron interactions and repulsive four-electron repulsive interactions in determining the structural effect of substituents in small-ring compounds.

Acknowledgment. This research has been supported by NSF Grants CHE 83-18188 at the University of Nebraska, CHE 86-04007 at Carnegie Mellon University, and CHE 81-08395 at the University of Kansas. T.D.N. acknowledges support of a Maude Hammond Fling Fellowship and a University of Nebraska Presidential Fellowship.

Registry No. **1**, 38693-83-3; **1-1-d**, 107383-60-8; **1-3-d**, 107383-61-9; **1-1-¹³C**, 107383-63-1; **1-4-¹³C**, 107383-64-2; **2**, 5500-21-0; **4**, 75-19-4; dimethyl phthalate, 131-11-3; dimethyl 3-*anti*-cyano-*exo*-tricyclo[3.2.2.0^{2,4}]nona-6,8-diene-6,7-dicarboxylate, 6254-43-9; dimethyl 3-*anti*-cyano-*exo*-tricyclo[3.2.2.0^{2,4}]nona-6,8-diene-6,7-dicarboxylate-3-*d*, 107383-62-0; dimethyl 3-*anti*-cyano-*endo*-tricyclo[3.2.2.0^{2,4}]nona-6,8-diene-6,7-dicarboxylate, 6204-44-0.

Velocity Modulation Laser Spectroscopy of Negative Ions: The ν_3 Band of Azide (N_3^-)

Mark Polak, Martin Gruebele, and Richard J. Saykally*

Contribution from the Department of Chemistry, University of California, Berkeley, California 94720. Received December 12, 1986

Abstract: Thirty-four transitions in the ν_3 (asymmetric stretch) fundamental of the azide anion have been measured in an NH_3/N_2O discharge by using diode laser velocity modulation spectroscopy. The data, ranging from P(42) to R(62), were fit to a linear molecule effective Hamiltonian through quartic terms. The vibrational band origin was determined to be $\nu_3 = 1986.4672$ (19) cm^{-1} and the rotational constants are $B'' = 0.426203$ (57) and $B' = 0.422572$ (55) cm^{-1} . Comparisons with ab initio calculations and condensed phase measurements are presented. The observed 2:1 intensity alternation in successive rotational lines establishes the centrosymmetric structure of the anion ($r_0 = 1.188402$ (82) Å).

The azide anion is of considerable importance in both organic and inorganic chemistry. For example, the reaction of the azide ion with carboxylic acids to form acyl azides has provided an essential precursor for the synthesis of amides and amines.¹ In transition-metal complexes, azide functions as a pseudohalide ligand, which can yield bridged as well as unidentate complexes.²

(1) Carey, F. A.; Sundberg, R. J. *Advanced Organic Chemistry Part B*; Plenum: New York, 1977; pp 329-31.

The detailed chemistry of azides is summarized in the text by Patai.³

All previous spectroscopic studies of azide have been carried out in condensed phases. N_3^- was observed in infrared and Raman

(2) Cotton, F. A.; Wilkinson, G. *Advanced Inorganic Chemistry*, 4th ed.; Wiley: New York, 1980; p 132.

(3) Patai, S. *The Chemistry of the Azido Group*; Interscience: London, 1971.

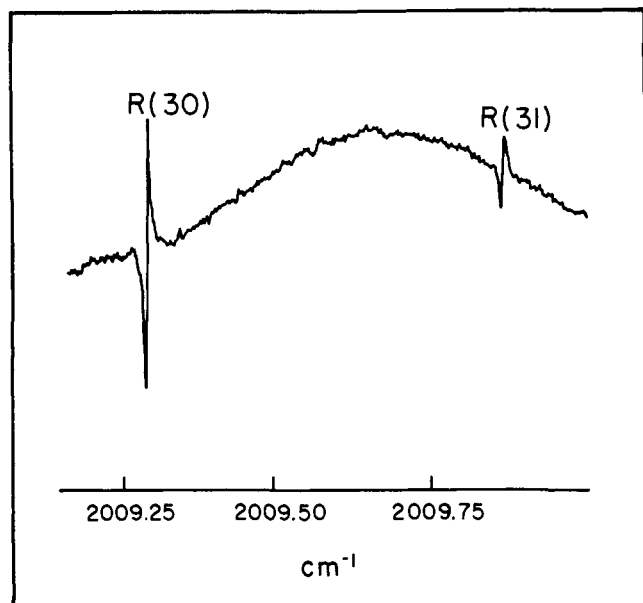


Figure 1. A representative scan showing the 2:1 intensity alternation. The alternation appears larger because of changes in laser power during the scan. The symmetries of the line shapes identify the transitions as negative ion absorptions.

studies of solutions and crystals as early as 1934.^{4,5} In solution, N_3^- was believed to have a linear centrosymmetric structure, while the solid-state spectra of both the symmetric and nonsymmetric structures have been observed. Subsequently there have been numerous such investigations of azide in a variety of condensed phase environments. By studying the effects of various crystal environments on N_3^- spectra, Sherman and Wilkinson⁶ have estimated the ν_3 vibrational frequency for the isolated N_3^- ion to be $1976 \pm 4 \text{ cm}^{-1}$. X-ray crystallographic studies have yielded N-N bond lengths in the range 1.12–1.16 Å.³

Recently, Botschwina⁷ has published a detailed theoretical calculation of the equilibrium structure and of the ν_1 and ν_3 stretching potentials of N_3^- . Of particular interest is the extraordinary transition strength ($\Gamma_3 = 66172 \text{ cm}^2 \text{ mol}^{-1}$) predicted for the ν_3 vibration (asymmetric stretch). This fundamental is 2–3 times stronger than the well-known and very strong ν_3 stretch of the isoelectronic CO_2 molecule. The prediction of the ν_3 band, near 1950 cm^{-1} , established our search region.

There have also been some gas-phase studies of the azide ion. Ilenberger et al.⁸ have determined the electron affinity of neutral N_3 to be $2.76 \pm 0.04 \text{ eV}$ through measurement of the photodetachment threshold of N_3^- . Azide has been observed by Bierbaum and co-workers^{9,10} as the dominant reaction product of NH_2^- and N_2O in flowing afterglows. As will be discussed below, we believe this to be the formation mechanism of N_3^- in our experiments as well.

The present work constitutes the first high-resolution spectroscopic detection of the azide anion and takes advantage of new developments in gas-phase molecular anion spectroscopy. Negative ions were first studied at high resolution by Lineberger and co-workers¹¹ by using photodetachment spectroscopy. Although this

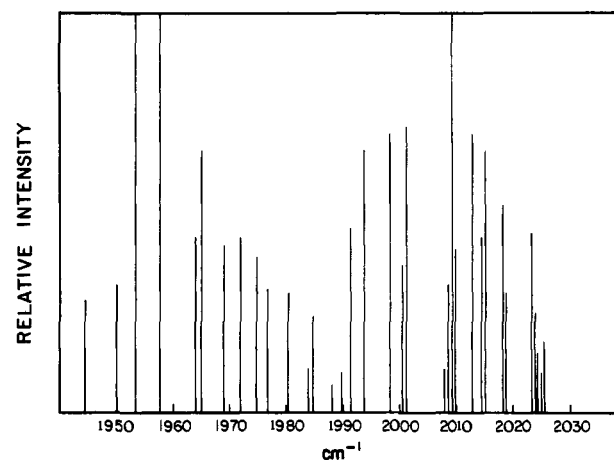


Figure 2. Computer reproduction of the observed lines in the ν_3 fundamental of N_3^- .

technique is extremely sensitive, rotational resolution is limited to light molecules or to ions with autodetaching states. Velocity modulated laser absorption spectroscopy provides a complementary high-resolution technique,¹² where detectability is limited only by the transition intensity and the ability to produce sufficient anion concentrations ($\sim 10^{10}$ molecules/cm³) in a positive column plasma. Negative ions studied thus far by direct absorption methods are OH^- ,¹³ OD^- ,¹⁴ NH_2^- ,¹⁵ FHF^- and FDH^- ,¹⁶ SH^- ,¹⁷ and C_2^- .¹⁸ The formation of some of these ions (OH^- , OD^- , and NH_2^-) is substantially enhanced by coating the discharge cell walls with metal, increasing anion concentrations by as much as a factor of 500.

Experimental Section

The experimental design has been described previously;¹⁹ only a brief outline will be presented here. Infrared radiation from a Laser Analytics tunable diode laser is single passed through a 1-m long 1-cm bore discharge cell driven at 25 kHz. Ion transitions are detected by their Doppler modulated absorption signals. The observed spectrum was readily attributed to a negative ion, because of the opposite symmetry of the first derivative line shapes relative to positive ion lines.¹³ Signal to noise ratios obtained ranged from 3 to 60 (Figure 1).

Optimum discharge conditions were 1.7 torr $NH_3/300$ mtorr N_2O . No detectable amounts of N_3^- were formed in pure NH_3 , pure N_2O , NH_3/O_2 , N_2O/H_2 , or NH_3/N_2 discharges. The use of helium and argon buffer gases decreased the signal. The N_3^- concentration was very sensitive to the discharge power and peaked upon operation just above the discharge breakdown voltage (1 kV at 400 W). Doubling of the discharge power decreased the signal by about a factor of ten. A similar power dependence was observed for NH_2^- ,¹⁵ although most of the ions observed in this laboratory have not shown a preference for low discharge power.

All measurements were done with copper sputtered on the walls of the discharge cell to increase negative ion production as first pointed out by Liu and Oka.²⁰ Subsequent cleaning of the cell showed that the N_3^- concentration was increased by a factor of 3–4 by the metal; however,

(4) Langseth, A.; Nielsen, J. R.; Sorenson, J. O. *Z. Phys. Chem. B* **1934**, *27*, 100–10.

(5) Sutherland, G. B. B. M.; Penney, W. G. *Proc. Roy. Soc. London A* **1936**, *156*, 678–86.

(6) Sherman, W. F.; Wilkinson, G. R. In *Vibrational Spectroscopy of Trapped Species*; Hallam, H. E., Ed.; Wiley: London, 1973; pp 245–354.

(7) Botschwina, P. *J. Chem. Phys.* **1986**, *85*, 4591–3.

(8) Ilenberger, E.; Comita, P. B.; Brauman, J. I.; Fenzlatt, H. P.; Heni, M.; Heinrich, N.; Koch, W.; Frenking, G. *Ber. Bunsen-Ges. Phys. Chem.* **1985**, *89*, 1026–31.

(9) Bierbaum, V. M.; Depuy, C. H.; Shapiro, R. H. *J. Am. Chem. Soc.* **1977**, *99*, 5800–2.

(10) Bierbaum, V. M.; Grabowski, J. J.; Depuy, C. H. *J. Phys. Chem.* **1984**, *88*, 1389–93.

(11) Neumark, D. M.; Lykke, K. R.; Andersen, T.; Lineberger, W. C. *J. Chem. Phys.* **1985**, *83*, 4364–73.

(12) Gudeman, C. S.; Saykally, R. *J. Ann. Rev. Phys. Chem.* **1984**, *35*, 387–418.

(13) Rosenbaum, N. H.; Owrutsky, J. C.; Tack, L. M.; Saykally, R. J. *J. Chem. Phys.* **1986**, *84*, 5308–13.

(14) Rehfuss, B. D.; Crofton, M. W.; Oka, T. *J. Chem. Phys.* **1986**, *85*, 1785–8.

(15) Tack, L. M.; Rosenbaum, N. H.; Owrutsky, J. C.; Saykally, R. J. *J. Chem. Phys.* **1986**, *85*, 4222–7.

(16) Kawaguchi, K.; Hirota, E. *J. Chem. Phys.* **1986**, *84*, 2953–60.

(17) Gruebele, M.; Polak, M.; Saykally, R. J. *J. Chem. Phys.* **1987**, *86*, 1698–1702.

(18) Rehfuss, B. D.; Liu, D.-J.; Dinelli, B. M.; Jayod, M.-F.; Crofton, M. W.; Oka, T. *41st Symposium on Molecular Spectroscopy, The Ohio State University*; 1986; paper WG2.

(19) Gruebele, M.; Polak, M.; Saykally, R. J. *J. Chem. Phys.* **1986**, *85*, 6276–81.

(20) Liu, D.-J.; Oka, T. *J. Chem. Phys.* **1986**, *84*, 2426–7.

Table I. Observed Transitions and Residuals from the Least-Squares Analysis

| line | freq | res | line | freq | res |
|-------|----------|------|-------|----------|------|
| P(42) | 1944.488 | 1.5 | R(14) | 1998.382 | -2.3 |
| P(37) | 1950.142 | -0.4 | R(17) | 2000.566 | -0.9 |
| P(34) | 1953.449 | 0.2 | R(18) | 2001.282 | -3.0 |
| P(30) | 1957.762 | -0.8 | R(28) | 2008.015 | 0.3 |
| P(24) | 1964.022 | -4.7 | R(29) | 2008.647 | 1.7 |
| P(23) | 1965.038 | -2.8 | R(30) | 2009.278 | -3.3 |
| P(19) | 1969.034 | 1.4 | R(31) | 2009.896 | -2.5 |
| P(16) | 1971.958 | 2.6 | R(36) | 2012.876 | 1.8 |
| P(13) | 1974.821 | 0.2 | R(39) | 2014.579 | 1.7 |
| P(11) | 1976.686 | 6.3 | R(40) | 2015.128 | 5.8 |
| P(7) | 1980.346 | 2.1 | R(46) | 2018.298 | 1.2 |
| P(3) | 1983.890 | -1.8 | R(47) | 2018.802 | -0.7 |
| P(2) | 1984.757 | -1.9 | R(57) | 2023.426 | -2.4 |
| R(1) | 1988.153 | -2.8 | R(58) | 2023.849 | -2.9 |
| R(3) | 1989.801 | 3.2 | R(59) | 2024.266 | -4.6 |
| R(5) | 1991.429 | 0.0 | R(61) | 2025.069 | 1.3 |
| R(8) | 1993.810 | 1.5 | R(62) | 2025.459 | 5.0 |

^a All frequencies are in cm^{-1} , and residual are in 10^{-3}cm^{-1} .

this is certainly an underestimate due to incomplete cleaning of the electrode towers.

Frequencies were measured to $\pm 0.003 \text{cm}^{-1}$ by using OCS,²¹ CO,²² and allene²³ as reference gases and with an oil bath stabilized Ge etalon for relative calibration. Approximate relative intensities were determined by using the etalon fringes as a measure of laser power. The difficulty in reproducing discharge conditions required that such intensity measurements be carried out in rapid succession. These measurements indicate an anomalously high rotational temperature for N_3^- , in excess of 1500 K. This interesting subject will be pursued in later studies.

Assignment and Analysis

A total of 34 lines has been assigned to the ν_3 fundamental (Figure 2). Because of the incomplete coverage of the diode laser, the rotational assignment presented some difficulty. All possible locations of the band origin could not be covered. Furthermore, populations of low J states were so small that the absence of a line at a possible band origin was insufficient evidence for assignment. Fortunately the 2:1 nuclear spin intensity alternation reduced possible assignments by a factor of two. Intensities from scans where two or more consecutive lines were observed yielded a tentative assignment. Possible rotational assignments were then limited to those resulting from shifts of $2J$ from the original one. Subsequent detection of R(1), R(3), R(5), and P(2), the absence of a line at the band origin, and the use of relative intensity measurements determined a unique assignment. The observed intensity alternation firmly established a linear centrosymmetric structure for N_3^- .

The measured transitions, ranging from P(42) to R(62), were fit with regression techniques to the standard linear molecule rotational Hamiltonian including quartic terms for the upper and lower states. Measured line positions and the residuals of the fit are given in Table I, and the parameters and correlation matrix from the least-squares fit are presented in Table II. From the ground-state rotational constant, the zero-point inverse rms N-N bond distance was determined, yielding $r_0 = 1.188402(82) \text{ \AA}$. Fitting the sextic centrifugal distortion term (H) did not significantly improve the standard deviation of the fit.

An additional 35 lines have also been observed, 25 of which have been tentatively assigned to the (011)-(010) hot band. These have not been completely analyzed, however, due to sparse data in the P-branch, and will be reported in a subsequent paper.

Discussion

A comparison of the experimental results with Botschwina's⁷ CEPA-1 ab initio calculations is given in Table III. In order to compare the equilibrium structure obtained from the calculation

Table II. Fitted Molecular Constants (cm^{-1}) for N_3^- ^a

| $\nu_3 = 1986.4672(19)$ | | | | |
|--|-------|-------|-------|-------|
| $B'' = 0.426203(57)$ | | | | |
| $D'' = 1.84(22) \times 10^{-7}$ | | | | |
| $B' = 0.422572(55)$ | | | | |
| $D' = 1.77(21) \times 10^{-7}$ | | | | |
| Correlation Matrix | | | | |
| ν_3 | B'' | D'' | B' | D' |
| 1.000 | | | | |
| 0.197 | 1.000 | | | |
| 0.172 | 0.914 | 1.000 | | |
| 0.158 | 0.999 | 0.910 | 1.000 | |
| 0.151 | 0.916 | 0.999 | 0.913 | 1.000 |
| Standard Deviation of Fit: 0.0029cm^{-1} | | | | |

^a All uncertainties are 2σ .

Table III. Comparison of Molecular Constants (cm^{-1})

| constant | N_3^- | | | N_3 ref 27 |
|-------------------------|----------------------------|--------------------|----------------------------|------------------------|
| | this work | ref 7 | other work | |
| r_0 (\AA) | 1.188402 (82) ^a | 1.195 ^b | (1.12 - 1.16) ^c | 1.185 |
| ν_3 | 1986.4672 (19) | 1950 | 1976 (4) ^d | |
| α_3 | 0.0036315 (35) | 0.00393 (20) | | |
| $D \times 10^7$ | 1.84 (22) (D_0) | 1.77 (9) (D_0) | | |

^a The following conversion factors and constants were used: I ($\text{ \AA}^2 \text{amu}$) = $16.876306/B$ (cm^{-1}) and m (nitrogen atom) = 14.00307439amu . ^b Estimation procedure from ab initio r_e described in discussion section. ^c X-ray crystallographic measurements quoted in ref 3. ^d Sherman and Wilkinson (ref 6).

with the zero-point structure determined experimentally, B_0 was estimated from Botschwina's B_e by

$$B_0 = B_e - \frac{1}{2}\alpha_1 - \alpha_2 - \frac{1}{2}\alpha_3$$

where α_1 and α_3 are from the calculation, and α_2 is estimated to be -0.0006cm^{-1} , the value for isoelectronic N_2O .²⁴ By using this estimation procedure, we obtain $r_0 = 1.195 \text{ \AA}$. Botschwina predicts that the calculated B_e value should be about 1% too low; adding 1% to his B_e value yields a zero-point N-N bond distance of 1.189 \AA , in excellent agreement with our result. The ab initio and experimental centrifugal distortion constants also show very good agreement.

The constants which directly involve the ν_3 potential, however, do not agree as well as the equilibrium parameters. The experimental value of α_3 falls just outside Botschwina's quoted uncertainty, and the theoretical value of ν_3 is 36cm^{-1} lower than experiment. Although the agreement with experiment is still good and Botschwina does suggest that ν_3 is slightly underestimated, the high level of theory used does not yield results as good as have been obtained for other negative ions, in particular for OH^- ²⁵ and NH_2^- .²⁶

Both theory and our results show a significant bond length increase in the isolated molecule relative to the X-ray crystallographic measurements (1.12 - 1.16 \AA).³ In addition, our experiment indicates only a slight increase in bond length from the neutral N_3 radical (1.1815 \AA), as measured by UV spectroscopy.²⁷ Since the additional electron in N_3^- goes into a nonbonding π orbital, only small changes between the neutral and ion structures are expected.

Table III also compares the estimates of the free ion properties made by Wilkinson and Sherman⁶ with our results. The estimate is based on spectroscopic observation of N_3^- as an impurity in a variety of different crystal hosts. The perturbing potentials of the crystals are assumed to be described by the Born-Mayer theory

(21) Hunt, N.; Foster, S. C.; Johns, J. W. C.; McKellar, A. R. W. *J. Mol. Spectrosc.* **1985**, *111*, 42-53.

(22) Guelachvili, G.; Rao, K. N. *Handbook of Infrared Standards*; Academic Press: Orlando, 1986; pp 492-535.

(23) Pliva, J.; Martin, C. A. *J. Mol. Spectrosc.* **1982**, *91*, 218-37.

(24) Guelachvili, G.; Amiot, C. *J. Mol. Spectrosc.* **1976**, *59*, 171-90.

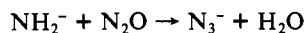
(25) Werner, H. J.; Rosmus, P.; Reinsch, E. A. *J. Chem. Phys.* **1983**, *79*, 905-16.

(26) Botschwina, P. *J. Mol. Spectrosc.* **1986**, *117*, 173-4.

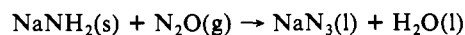
(27) Douglas, A. E.; Jones, W. J. *Can J. Phys.* **1965**, *43*, 2216-21.

of ionic crystals,²⁸ and the experimental results are extrapolated to the unperturbed free ion. The excellent agreement of the vibrational frequency obtained in this manner ($1976 \pm 4 \text{ cm}^{-1}$) with the frequency obtained in these gas-phase experiments seems to indicate a good understanding of lattice perturbations of this negative ion; however, a more extensive set of gas-phase data is clearly needed to show that the agreement is as good for other molecular anions.

While theoretical and low-resolution spectroscopic predictions guided the search for the ν_3 vibrational spectrum, previous chemical studies helped determine optimum chemistry for N_3^- production. In their flowing afterglow apparatus, Bierbaum et al.¹⁰ have observed that the gas-phase reaction



occurs with an efficiency of 72% and a second-order rate constant of $2.9 \times 10^{-10} \text{ cm}^3 \text{ molecule}^{-1} \text{ s}^{-1}$. Interestingly, this is the gas phase analogues of the reaction



which is used extensively in large scale industrial production of azides.³ Since Tack et al.¹⁵ observed large concentrations ($4 \times 10^{11} \text{ molecules/cm}^3$) of the amide ion in pure ammonia discharges, it was predicted that adding N_2O to an ammonia discharge would result in formation of azide. As predicted, N_3^- was formed in a

1.7 torr $\text{NH}_3/300 \text{ mtorr N}_2\text{O}$ discharge. As in the NH_2^- study, enhancement of negative ion production by the presence of a metal coating on the discharge cell walls was found, as was a preference for low discharge power. Furthermore, all discharges found to produce detectable amounts of N_3^- contained both NH_3 and N_2O . This clearly indicates that the most likely mechanism for azide formation is the $\text{NH}_2^-/\text{N}_2\text{O}$ reaction. Because of the strong basicity¹⁰ and relatively low electron binding energy (0.744 eV)²⁹ of the amide ion, ammonia discharges may prove useful in the gas-phase production of other negative ions as well.

As mentioned previously, 25 lines have been tentatively assigned to the (011)-(010) hot band of N_3^- . Complete analysis awaits an improvement of our diode laser coverage in the region of the P-branch. In addition, we will search for the (101)-(000) combination band, which is predicted⁷ to be quite strong ($\Gamma_1 = 1512 \text{ cm}^2/\text{mol}$) and to be located at 3211 cm^{-1} . This combination of data should lead to the first experimental determination of the equilibrium structure of a polyatomic negative ion.

Acknowledgment. This work was supported by the National Science Foundation (Grant No. CHE 8402861) and by a grant from the IBM Corporation through the NSF Presidential Young Investigator program. We thank Peter Botschwina for providing results before publication and Veronica M. Bierbaum for helpful advice concerning ion chemistry. M.G. thanks IBM for a Graduate Research Fellowship.

(28) Born, M.; Mayer, J. E. *Z. Physik* 1932, 75, 1-18.

(29) Smyth, K. C.; Brauman, J. I. *J. Chem. Phys.* 1972, 56, 4620-5.

Chirality Forces

Lionel Salem,* Xavier Chapuisat, Gerald Segal,¹ Philippe C. Hiberty, Christian Minot, Claude Leforestier, and Philippe Sautet

Contribution from the Laboratoire de Chimie Théorique (UA 506), Université de Paris-Sud, 91405 ORSAY Cedex, France. Received July 28, 1986

Abstract: The differential interaction energy between two chiral tetrahedral molecules, first with the same chirality (homochiral, $R \leftrightarrow R'$) and second with opposite chirality (heterochiral, $R \leftrightarrow S'$), is analyzed in the limit of free relative molecular rotation (high-temperature limit, interactions small relative to kT). This differential energy measures the degree of "chiral recognition" or "chiral discrimination". It is shown that, if the energy of interaction is expressed as a sum of interactions between atomic centers on the two molecules, *six-center* forces, occurring simultaneously between triplets of atoms, one triplet in each molecule, are responsible for the discrimination. Since this is the first natural phenomenon where six-center forces are found to play an important role we call these forces *chirality forces*. Models which are based on two-center forces alone (charges on the four atoms) or four-center forces (dipoles on the tetrahedron edges) fail to give any chiral discrimination in the freely rotating limit. A model based on the *simultaneous* overlap-exchange interaction between three pairs of centers on the two molecules does yield a discrimination after averaging freely over all relative orientations. The energy preference is found to be $0.5 \cdot 10^{-2} - 10^{-4}$ times the total rotationally averaged interaction energy at a distance of 5 Å. Two pyramidal chiral ammonia molecules (hydrogens with different exponents) interacting face-to-face at 4 Å also have an average SCF discrimination of 9.2 small J/mol for their eclipsed configurations. Comparison is made with the Boltzmann-weighted discrimination due to direct two-center net charge-net charge interactions. Third-order dispersion forces, which also contribute to the chiral discrimination between interacting tetrahedra, are discussed and compared with the six-center chirality forces.

1. Introduction

Surprising as it may seem, the asymmetric nature of tetrahedral carbon has been recognized for more than a century,² and yet no attempt has been made to evaluate the interaction energy between

two asymmetric tetrahedral molecules. In several important papers^{3a-c} and in an exhaustive review^{3d} Craig and co-workers have examined the discriminating interactions between chiral molecules.

(1) On leave from the Department of Chemistry, University of Southern California, Los Angeles, CA 90007.

(2) (a) Le Bel, J. A. *Bull. Soc. Chim. Fr.* 1874, 22, 337. (b) van't Hoff, J. H. *Arch. Neerland. Sci. Exact. Nat.* 1874, 9, 445.

(3) (a) Craig, D. P.; Power, E. A.; Thirunamachandran, T. *Proc. Roy. Soc. London* 1971, A322, 165. (b) Craig, D. P.; Schipper, P. E. *Proc. Roy. Soc. London* 1975, A342, 19. (c) Craig, D. P.; Radom, L.; Stiles, P. J. *Proc. Roy. Soc. London* 1975, A343, 11. (d) Craig, D. P.; Mellor, D. P. *Topic Curr. Chem.* 1976, 63, 1. (e) Craig, D. P. In *Optical Activity and Chiral Discrimination*; Mason, S. F., Ed.; Reidel: Dordrecht, 1979; p 310.